Electronic Supporting Information for

Conformationally Dynamic Copper Coordination Complexes

Bronte J. Charette, Paul J. Griffin, Claire M. Zimmerman and Lisa Olshansky*
Department of Chemistry, University of Illinois at Urbana-Champaign, Urbana, Illinois, 618081, United States

Table of Contents

VT-NMR lineshape analysis was performed using equations derived from Bloch equations modified to include a pseudo-first order decay term.[1,2] Each signal was fit to a Lorentzian shape in MestReNova Software.[3] Using an estimation of the transverse relaxation (T_2^{eff}) in the absence of exchange from the full width at half max (fwhm) of a non-exchanging proton signal (equation 1), the pseudo-first order rate constant (k) can be calculated from the fwhm for the subsequent signal (Eq 2).

$$T_2^{eff} = \frac{1}{\pi\,[fwhm]} \tag{1}$$

$$k = \pi[fwhm - \frac{1}{\pi T_2^{eff}}] \tag{2}$$

Following determination of k, a plot of ln(k/T) versus 1/T was used to extract activation parameters using the following equations:

$$ln\left(\frac{k}{T}\right) = \frac{\Delta H^{\ddagger}}{R} * \frac{1}{T} + \ln\left(\frac{k_b}{h}\right) + \frac{\Delta S^{\ddagger}}{R} \tag{3}$$

Where:

$$Slope = \frac{\Delta H^{\ddagger}}{R} \tag{4}$$

$$Intercept = \ln\left(\frac{k_b}{h}\right) + \frac{\Delta S^{\ddagger}}{R} \tag{5}$$

Constants used:
$k_b = 1.38 \times 10^{-23}$ J-K^{-1}
$h = 6.63 \times 10^{-34}$ J-s
R = 1.98 cal K^{-1}-mol^{-1}

Table S1. EPR simulation parameters for [CuCl(dpa^{OMe})][PF_6].

	$g_\perp$ 2.04	$g_{||}$ 2.25	
Cu	24	464	MHz
N(1)	48	5	MHz
N(2)	47	11	MHz
N(3)	40	8	MHz

Table S2. EPR simulation parameters for $CuCl_2$(dpa^{H}).

	g_1 2.02	g_2 2.12	g_3 2.25	
Cu	51	130	437	MHz
N(1)	58	54	25	MHz
N(2)	60	55	35	MHz
N(3)	59	55	30	MHz

Table S3. Peak[a] integrations obtained from DPV for CuCl(dpa^{OMe}) and CuCl(dpa^{H}).

CuCl(dpa^{OMe})			CuCl(dpa^{H})		
	$E_{p1}^{\circ'}$	$E_{p2}^{\circ'}$		$E_{p1}^{\circ'}$	$E_{p2}^{\circ'}$
1.4 mM	9.17×10^{-7}	9.33×10^{-7}	0.6 mM	6.37×10^{-7}	7.67×10^{-7}
2.8 mM	1.62×10^{-6}	1.30×10^{-6}	1.2 mM	1.36×10^{-6}	9.14×10^{-7}
7.0 mM	2.87×10^{-5}	1.72×10^{-6}	5.0 mM	2.39×10^{-6}	1.04×10^{-6}

[a] $E_{p1}^{\circ'}$ and $E_{p2}^{\circ'}$ refer to the oxidative peak potentials measured by DPV.

Table S4. Parameters obtained from simulated CVs of CuCl(dpa^{OMe}) and [CuCl(dpa^{OMe})]$^{+}$.

	CuCl(dpa^{OMe})		[CuCl(dpa^{OMe})][PF_6]	
	$E_1^{\circ'}$	$E_2^{\circ'}$	$E_1^{\circ'}$	$E_2^{\circ'}$
V vs $Fc^{+/0}$ [a]	–0.56	–0.01	–0.59	–0.01
K_{eq}	125 [b]	0.65 [c]	--	0.007[c]
k_s /cm^{-1} [d]	0.016	0.006	0.011	10
k_f /s^{-1} [e]	0.01	8 x10^{-5}	--	0.07
k_r /s^{-1} [f]	0.1	0.15	--	10
α [g]	0.5	0.5	0.5	0.5
R_u / Ω [h]	100	100	100	100
C_{dl} / μF [i]	1 ×10^{-5}	1 ×10^{-6}	1 × 10^{-5}	1 × 10^{-5}
D /cm^2 s^{-1} [j]	8 × 10^{-6}	8 × 10^{-6}	1.1 ×10^{-5}	1.1 × 10^{-5}

Table S5. Parameters obtained from simulated CVs of CuCl(dpa^{H}) and $CuCl_2$(dpa^{H}).

	CuCl(dpa^{H})		$CuCl_2$(dpa^{H})	
	$E_1^{\circ'}$	$E_2^{\circ'}$	$E_1^{\circ'}$	$E_2^{\circ'}$
V vs $Fc^{+/0}$ [a]	–0.44	–0.04	–0.47	–0.06
K_{eq}	125 [b]	0.4 [c]	1.5 x10^{-4} [b]	9.5 x10^{-4} [c]
k_s /cm^{-1} [d]	0.015	0.004	0.017	0.005
k_f /s^{-1} [e]	0.01	8 x10^{-5}	0.08	533
k_r /s^{-1} [f]	0.1	0.26	0.017	17.8
α [g]	0.5	0.5	0.5	0.5
R_u / Ω [h]	100	100	100	100
C_{dl} / μF [i]	1 ×10^{-5}	1 ×10^{-5}	1 ×10^{-5}	1 ×10^{-5}
D /cm^2 s^{-1} [j]	8.5 ×10^{-6}	8.5 ×10^{-6}	1.5 ×10^{-5}	1.5 ×10^{-5}

[a]Redox potential. [b]Equilibrium constant for the dynamic process in the copper (II) state. [c]Equilibrium constat for the dynamic process in the copper (I) state. [d]Rate constant for the electron transfer. [e]Rate constant for the dynamic process in the copper (II) state. [f]Rate constant for the dynamic process in the copper (I) state. [g]Electron transfer coefficient. [h]Resistance. [i]Capacitance. [j]Diffusion coefficient for all species.

Table S6. XRD collection and refinement parameters for [{Cu(dpa^{OMe})}$_2$(μ-Cl)][CuCl$_2$] and [CuCl(dpa^{OMe})][PF$_6$].

	[{Cu(dpa^{OMe})}$_2$(μ-Cl)][CuCl$_2$]	[CuCl(dpa^{OMe})][PF$_6$]•2CH$_2$Cl$_2$
empirical formula	$C_{38}H_{38}Cl_3Cu_3N_6O_2$	$C_{21}H_{23}Cl_5CuF_6N_3OP$
formula weight	907.71	719.18
crystal system	orthorhombic	triclinic
space group	$P2_12_12_1$	$P\bar{1}$
T(K)	130.0	100.0
a / Å	8.2127(2)	10.4034(6)
b / Å	19.9564(5)	11.1847(7)
c / Å	23.1694(6)	13.3875(7)
α / deg	90	72.920(2)
β / deg	90	69.922(2)
γ / deg	90	78.631(2)
V / Å^3	3797.37(17)	1390.49(14)
Z	4	2
refl. collected	28242	50210
indep. refl.	7769 [R(int) = 0.0453]	5716 [R(int) = 0.0399]
R1 ($I > 2\sigma$)[a]	0.0295(0.0356)	0.0472 (0.0550)
*w*R2 (all data)[b]	0.0570(0.0596)	0.1249 (0.1336)
GOF	1.054	1.055

[a] $R1 = \Sigma||F_o|-|F_c||/\Sigma|F_o|$; [b] $wR2 = [\Sigma[w(F_o^2-F_c^2)^2]/\Sigma[w(F_o^2)^2]]^{½}$

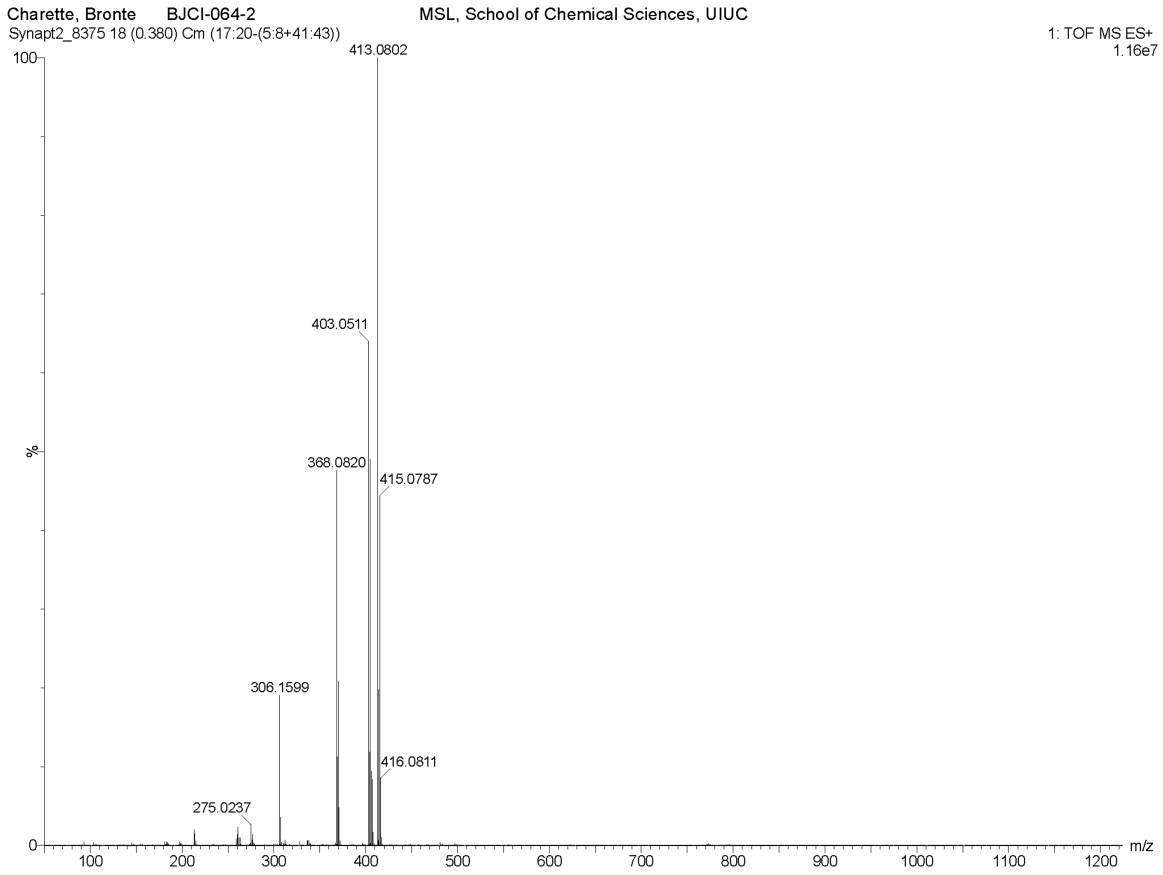

Figure S1. Mass spectrum of CuCl(dpa^{OMe}) in DCM.

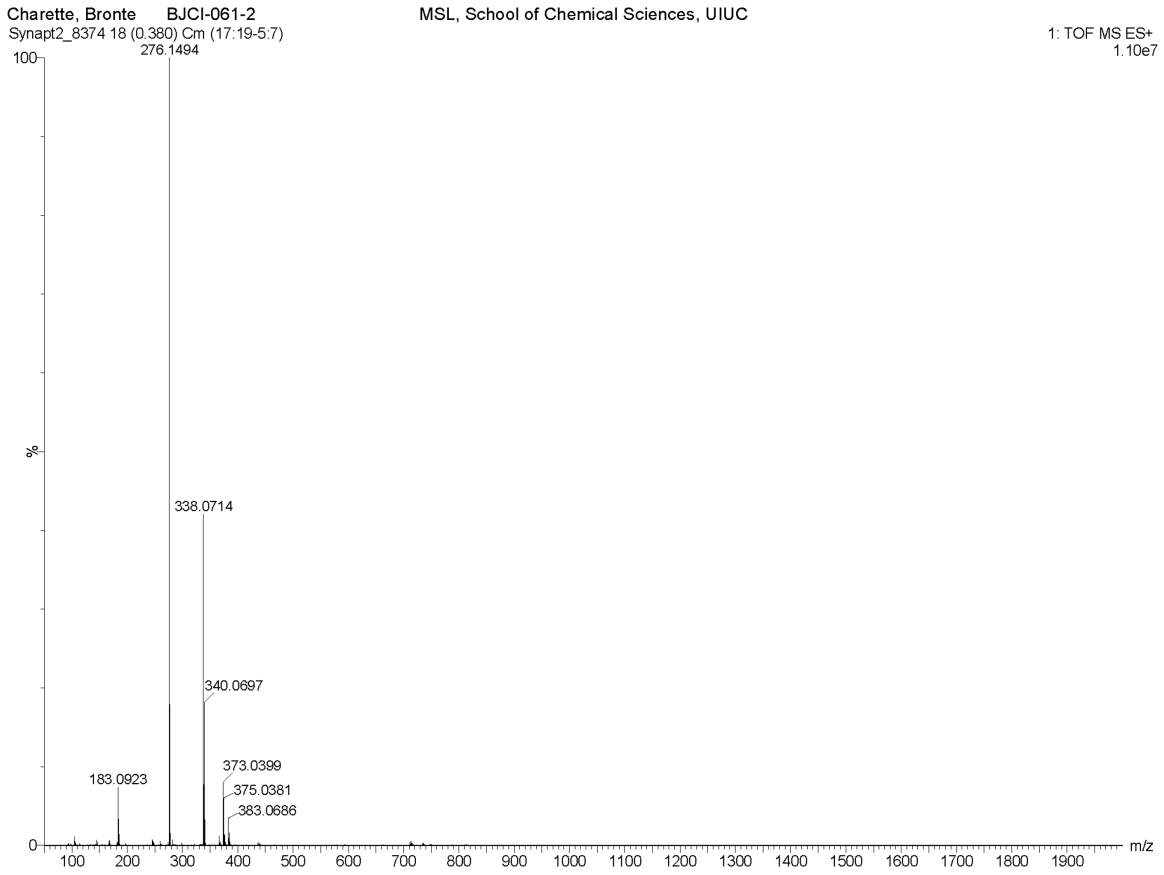

Figure S2. Mass spectrum of CuCl(dpa^{H}) in DCM.

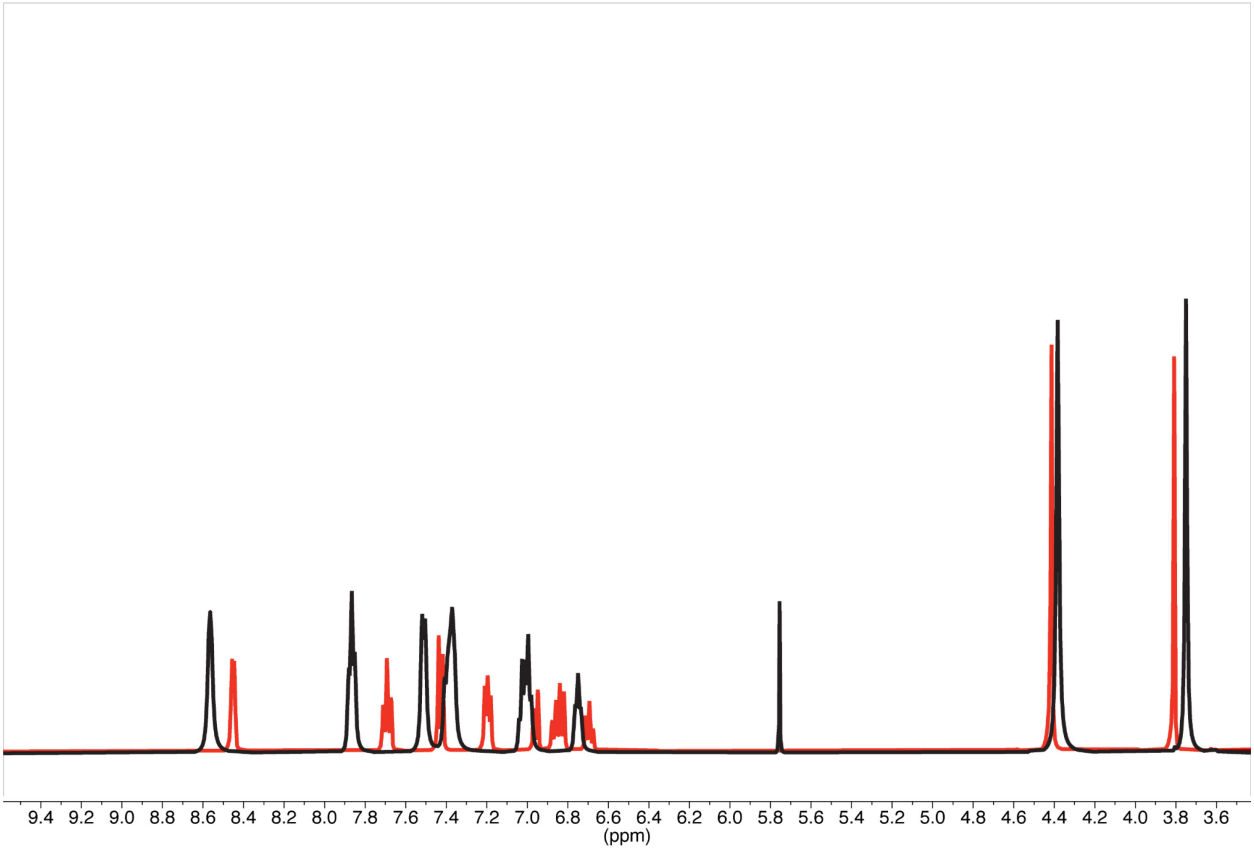

Figure S3. Overlayed ^{1}H-NMR spectrum of CuCl(dpa^{OMe}) (black) and dpa^{OMe} ligand (red) in d_6-DMSO at 298 K.

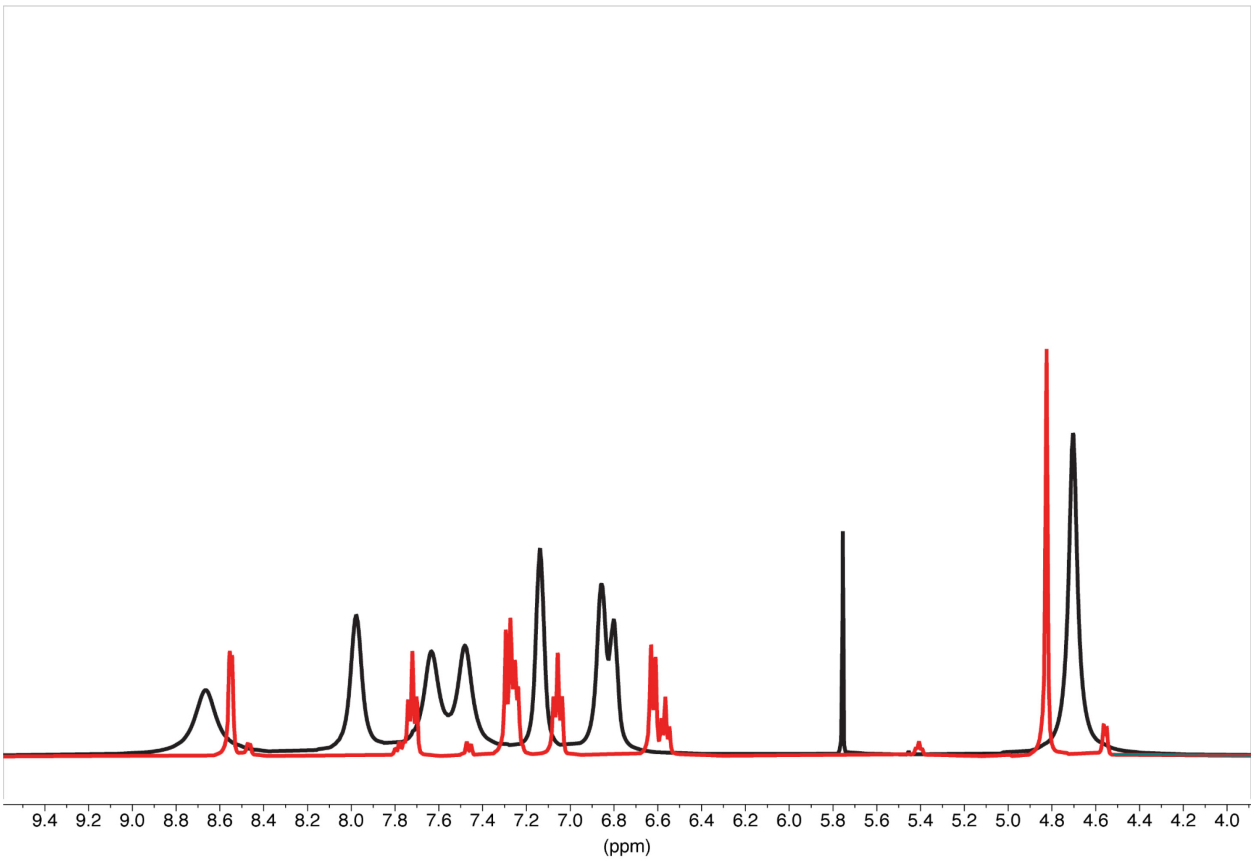

Figure S4. Overlayed ^{1}H-NMR spectrum of CuCl(dpa^{H}) (black) and dpa^{H} ligand (red) in d_6-DMSO at 298 K.

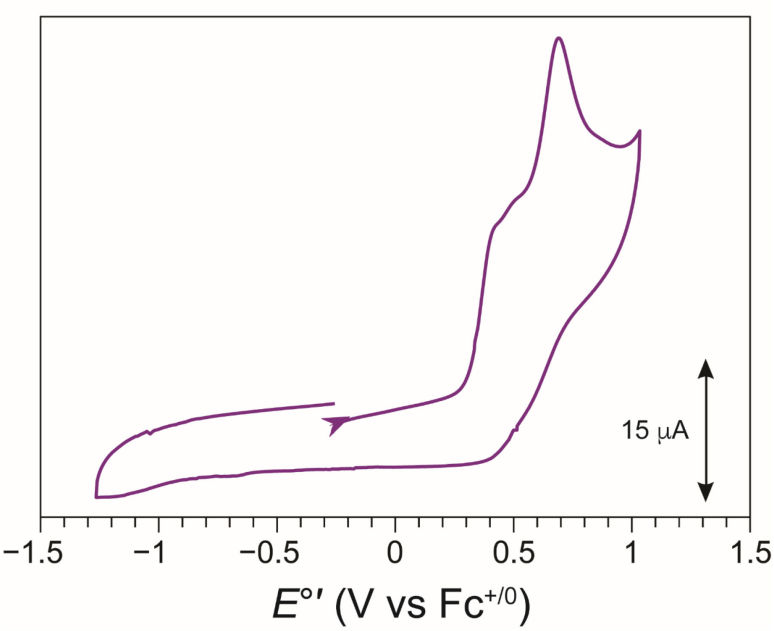

Figure S5. CV recorded with 1 mM ligand dpa^{OMe} concentration with 100 mM $[NBu_4][PF_6]$ electrolyte in dry degassed DMF under a nitrogen atmosphere using a 3 mm glassy carbon working electrode, Pt wire counter electrode and $Ag^{+/0}$ pseudo-reference electrode at room temperature with 100 mVs^{-1} scan rate.

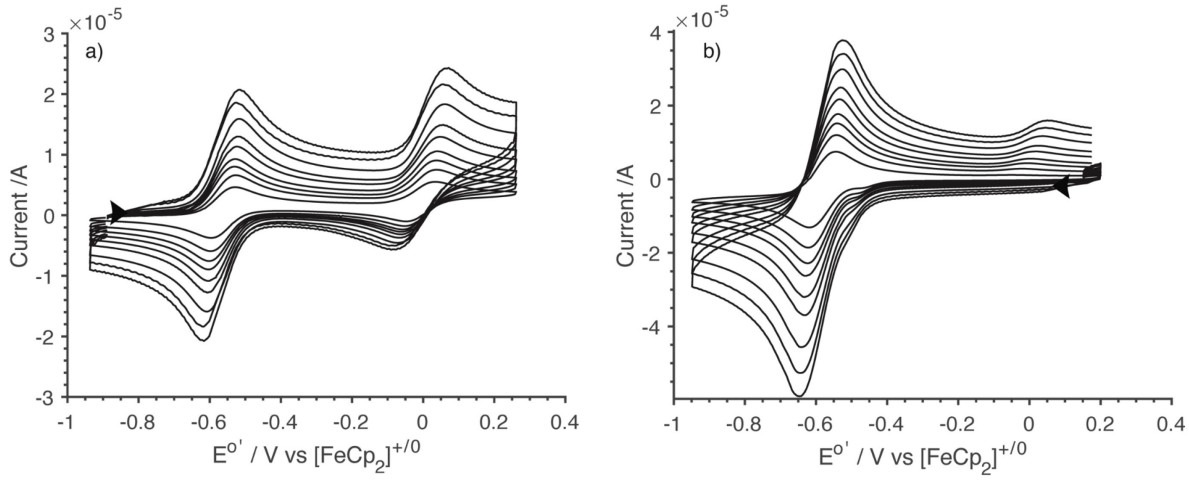

Figure S6. CV scan rate dependencies of a) CuCl(dpa^{OMe}) and b) [CuCl(dpa^{OMe})][PF_6] at 25, 50, 75, 100, 150, 200, 300, 400 and 500 mV sec^{-1} scan rates. Cyclic voltammograms were recorded with 1 mM analyte and 100 mM [NBu_4][PF_6] electrolyte in dry degassed DMF under a nitrogen atmosphere using a 3 mm glassy carbon working electrode, Pt wire counter electrode and $Ag^{+/0}$ pseudo-reference electrode at ambient temperature.

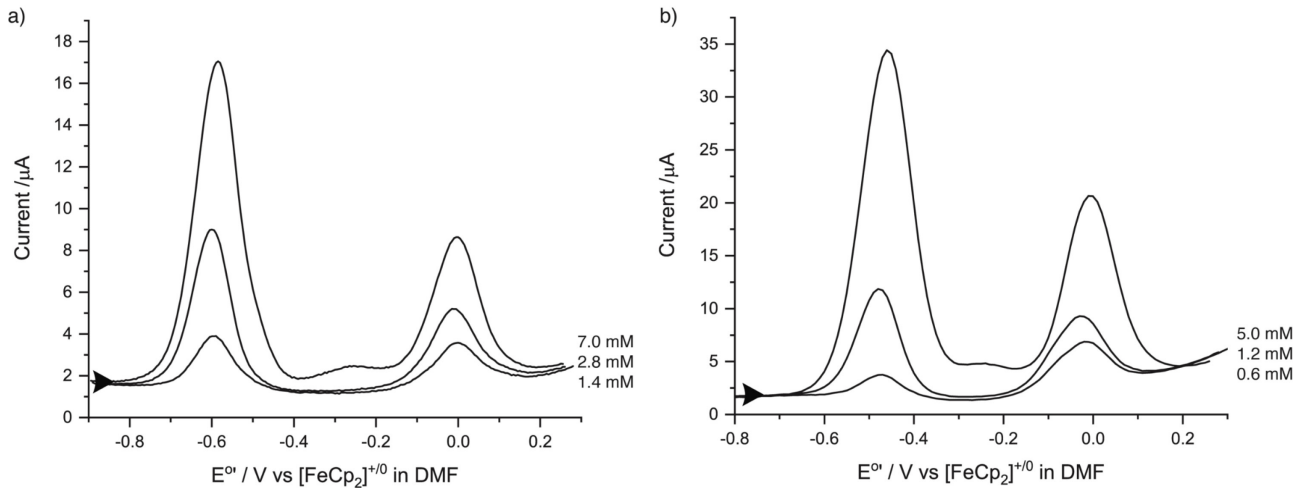

Figure S7. Differential pulse voltammograms for a) CuCl(dpa^{OMe}) at 1.4 mM, 2.8 mM and 7.0 mM concentrations and b) CuCl(dpa^{H}) at 0.6 mM, 1.2 mM and 5 mM in DMF at ambient temperatures. Data were collected using the same solution conditions to cyclic voltammograms.

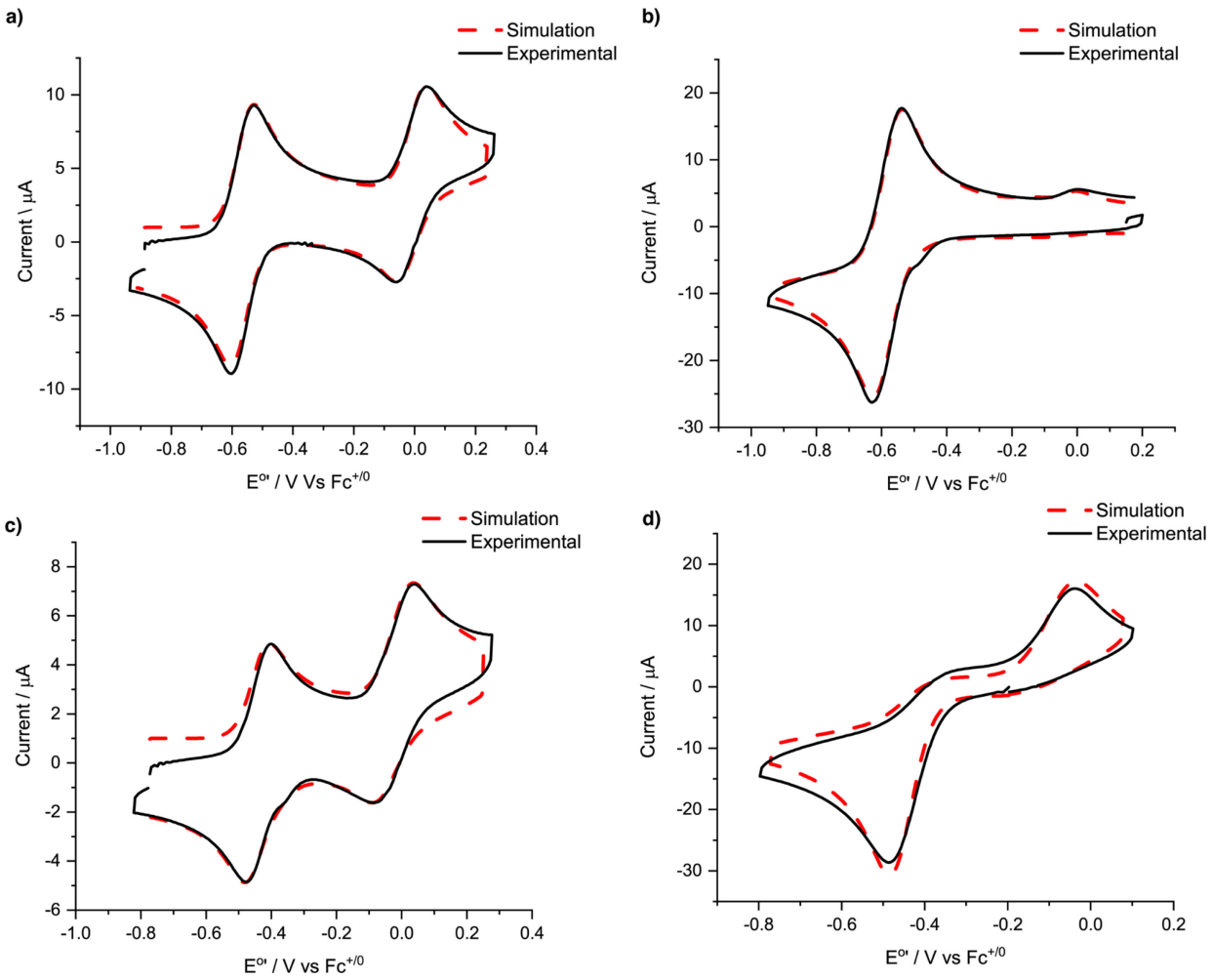

Figure S8. CV simulations on 1 mM solutions of a) CuCl(dpa^{OMe}), b) [CuCl(dpa^{OMe})][PF_6], c) CuCl(dpa^{H}) and d) $CuCl_2$(dpa^{H}) performed using BASi DigiElch 8.0 with simulated spectra in red dashed lines and experimental spectra in black solid lines.

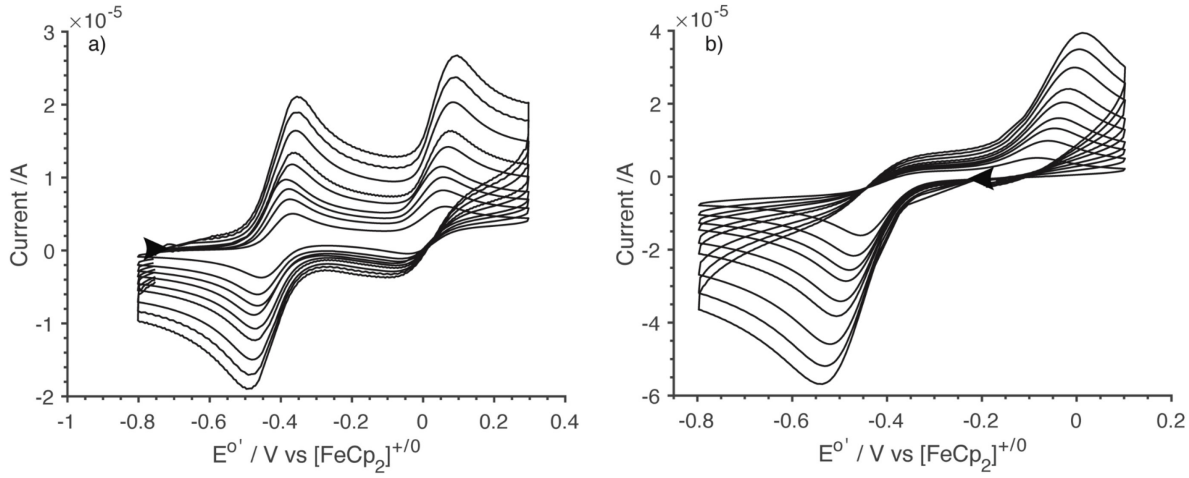

Figure S9. CV scan rate dependencies of a) $CuCl(dpa^{H})$ and b) $CuCl_2(dpa^{H})$ at 25, 50, 75, 100, 150, 200, 300, 400 and 500 mV sec^{-1} scan rates. Cyclic voltammetry were recorded with 1 mM analyte concentration with 100 mM $[NBu_4][PF_6]$ electrolyte in dry degassed DMF under a nitrogen atmosphere using a 3 mm glassy carbon working electrode, Pt wire counter electrode and $Ag^{+/0}$ pseudo-reference electrode at ambient temperature.

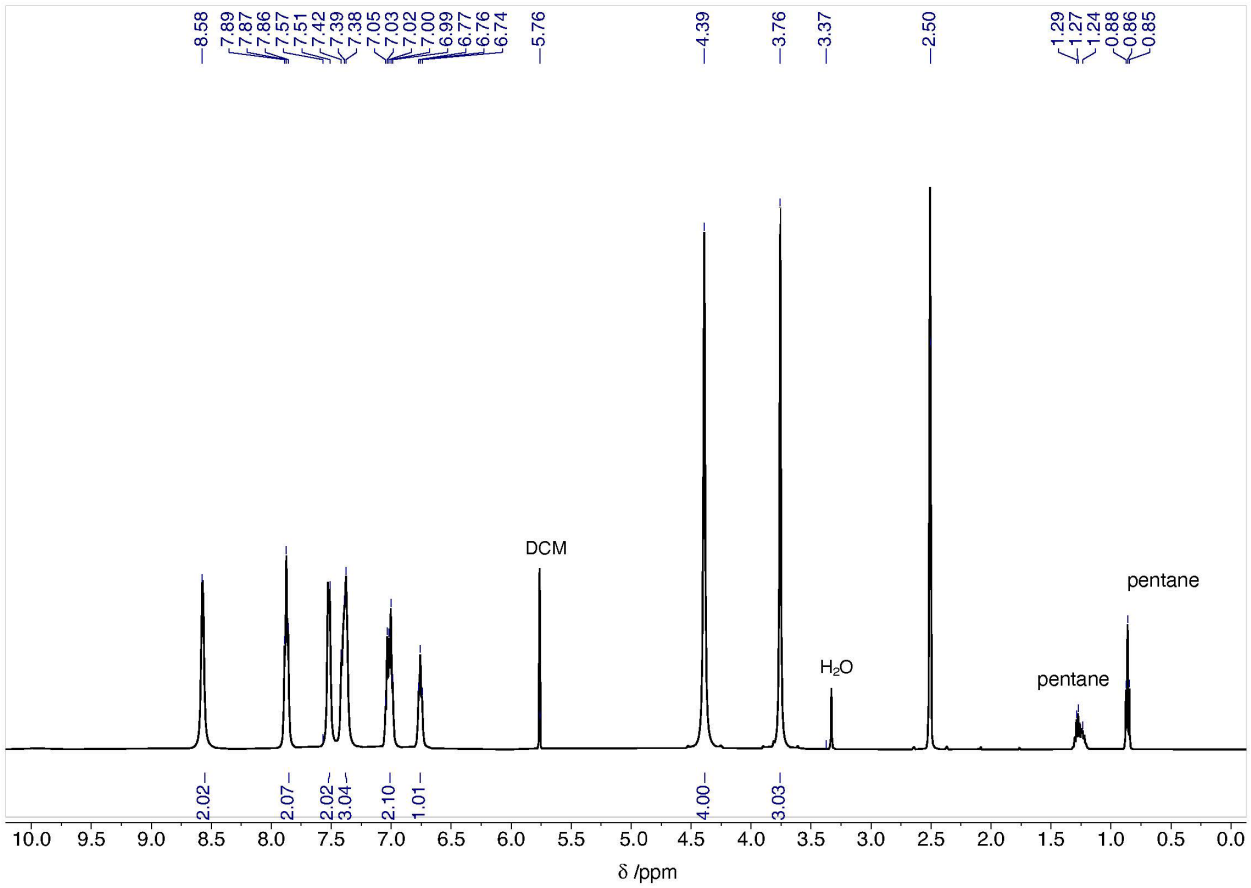

Figure S10. ^{1}H-NMR spectrum of CuCl(dpa^{OMe}) in d_6-DMSO at 298 K.

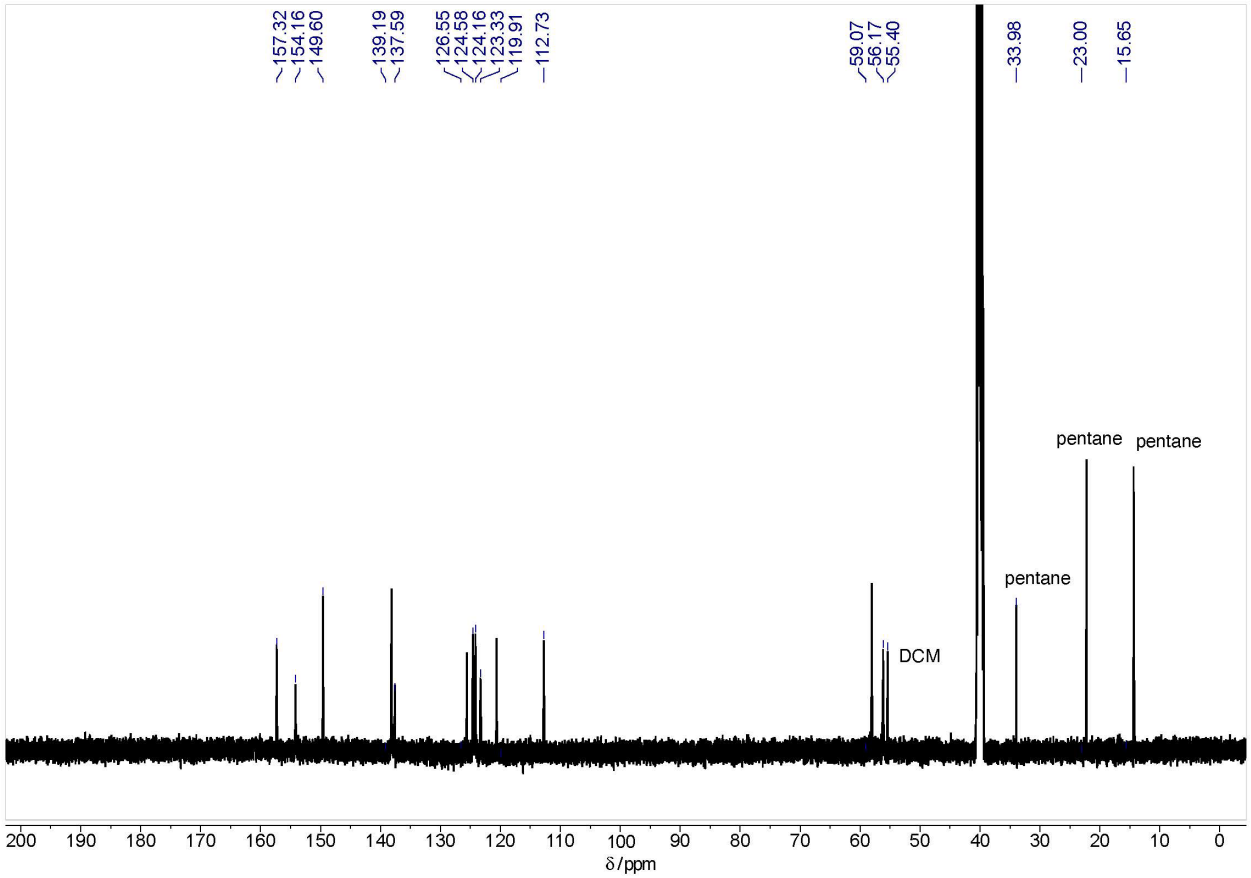

Figure S11. ^{13}C-NMR spectrum of CuCl(dpa^{OMe}) in d_6-DMSO at 298 K.

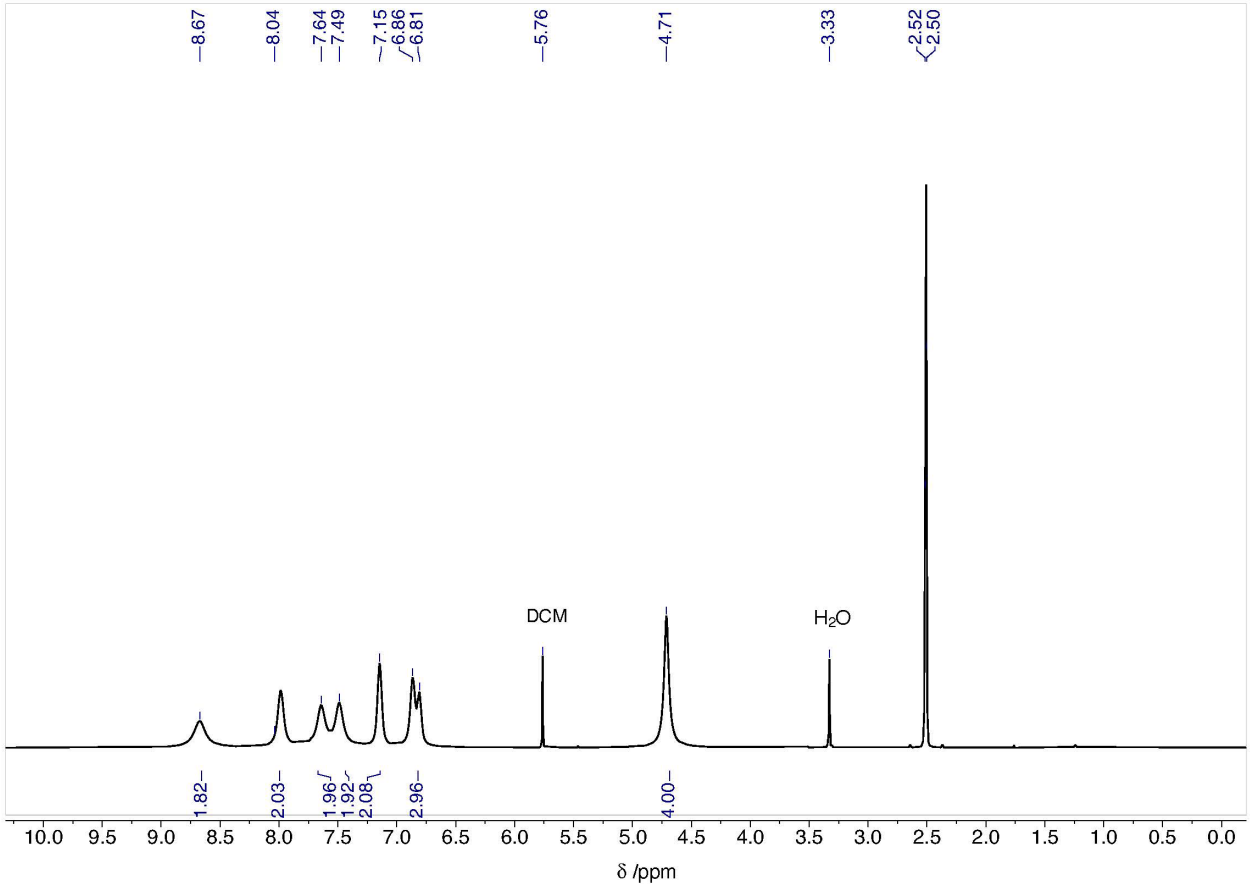

Figure S12. ^{1}H-NMR spectrum of CuCl(dpa^{H}) in d_6-DMSO at 298 K.

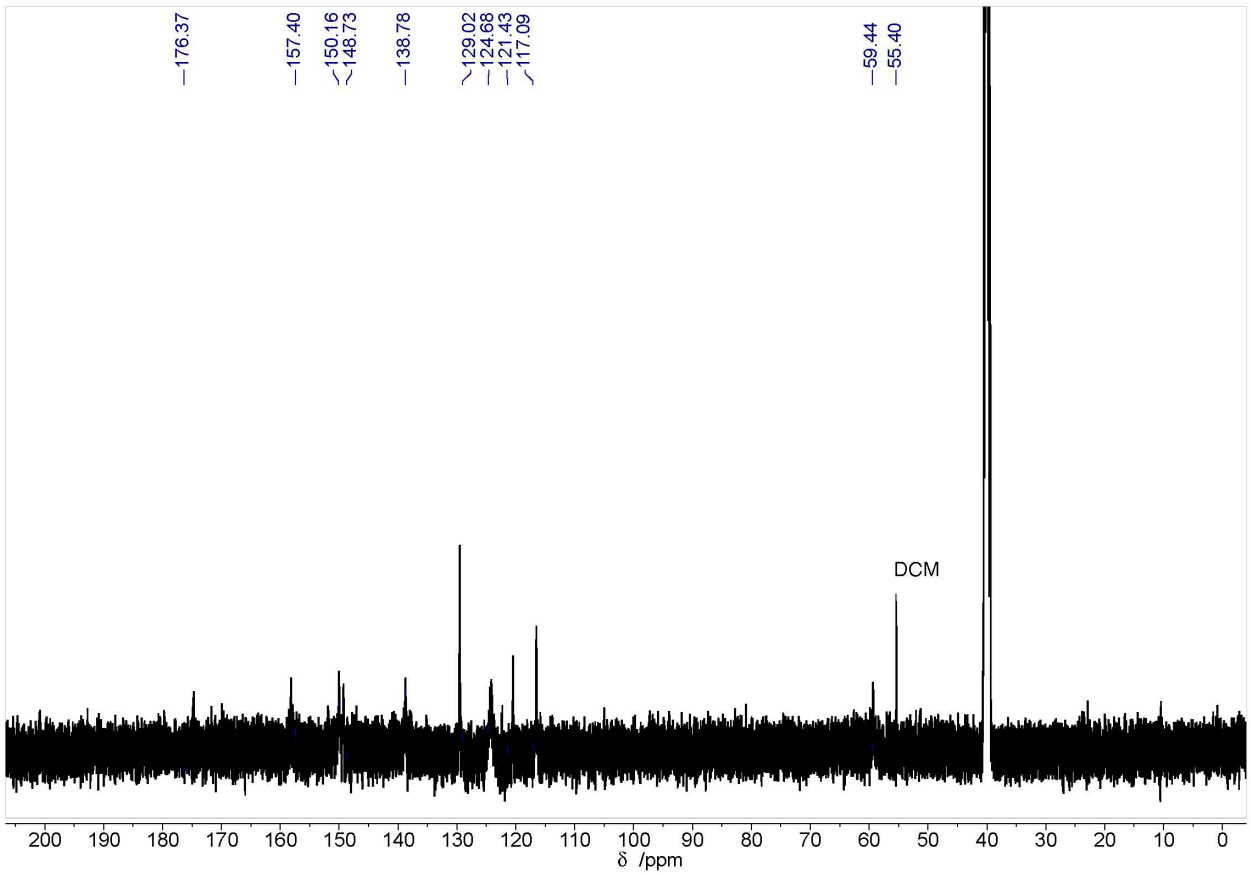

Figure S13. ^{13}C-NMR spectrum of CuCl(dpa^{H}) in d_6-DMSO at 298 K.

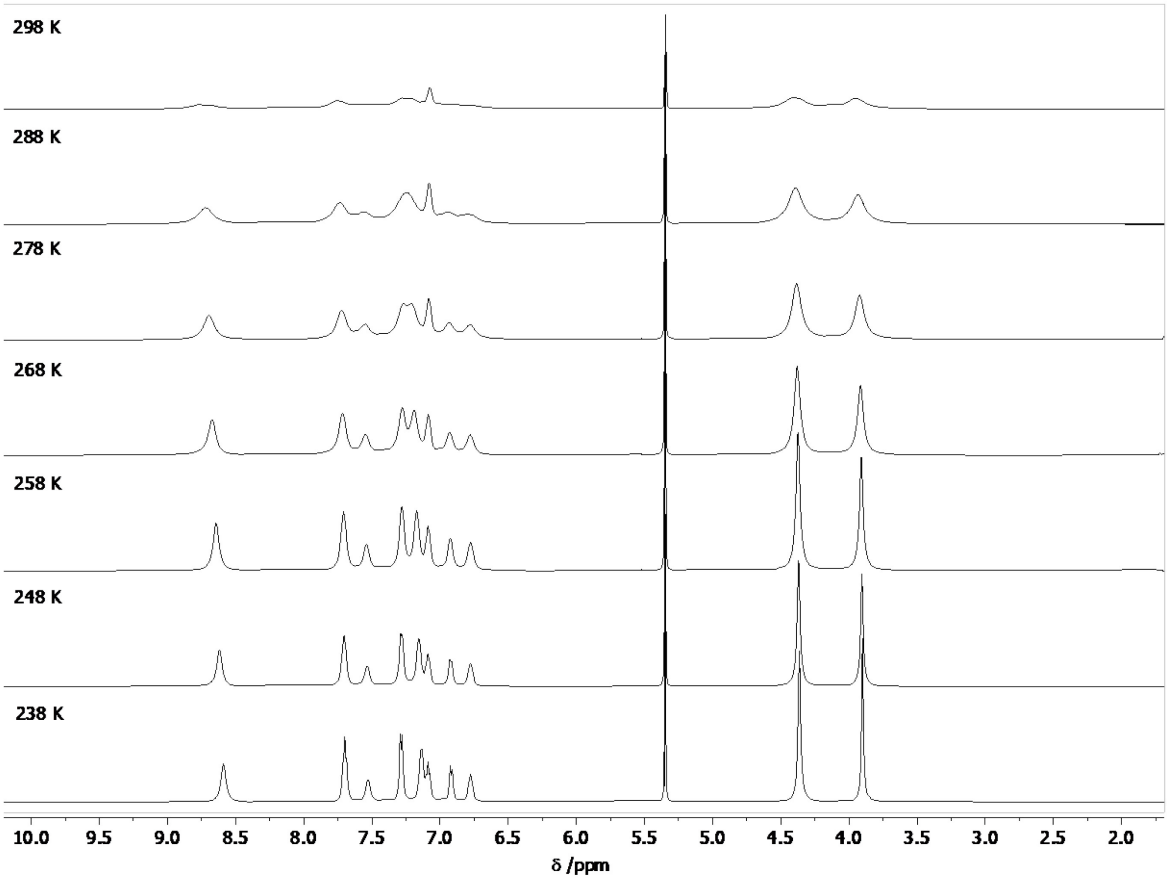

Figure S14. ^{1}H-NMR spectra (500 MHz) of CuCl(dpa^{OMe}) in d_2-DCM over the temperature range of 238-298 K.

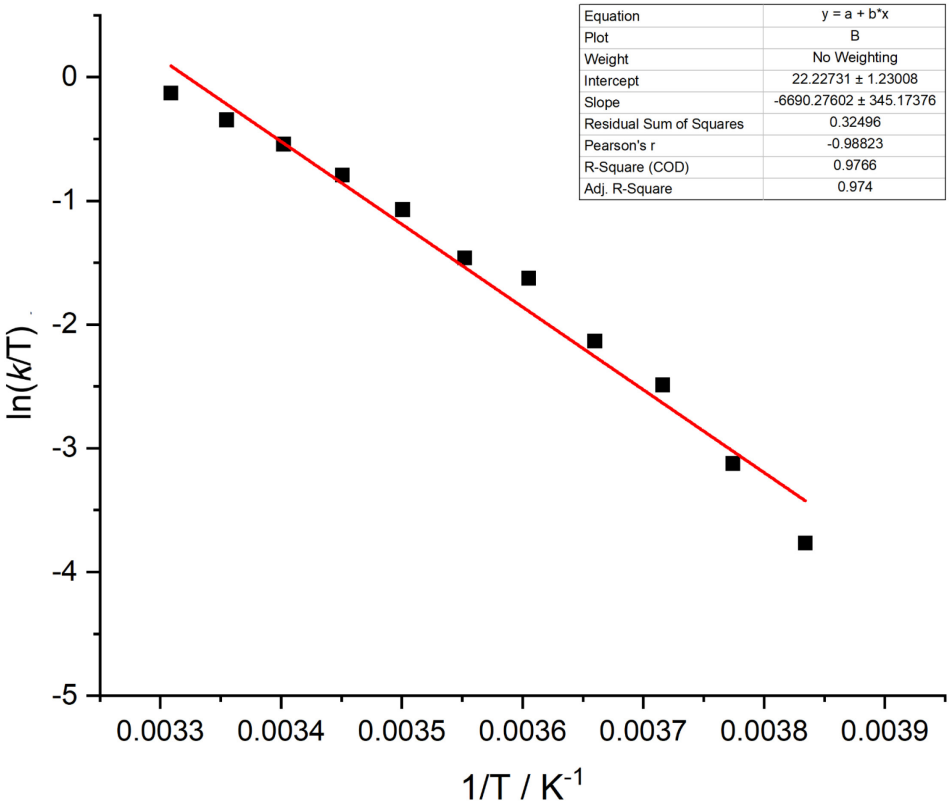

Figure S15. Plot of ln(k/T) versus 1/T (where k = rate constant and T = temperature in K) for the dynamic NMR process of CuCl(dpa^{OMe}) in d_2-DCM from 238-298 K. The shown linear fit was used to calculate the activation parameters listed in the main text via the Eyring equation (R^2 = 0.9766).

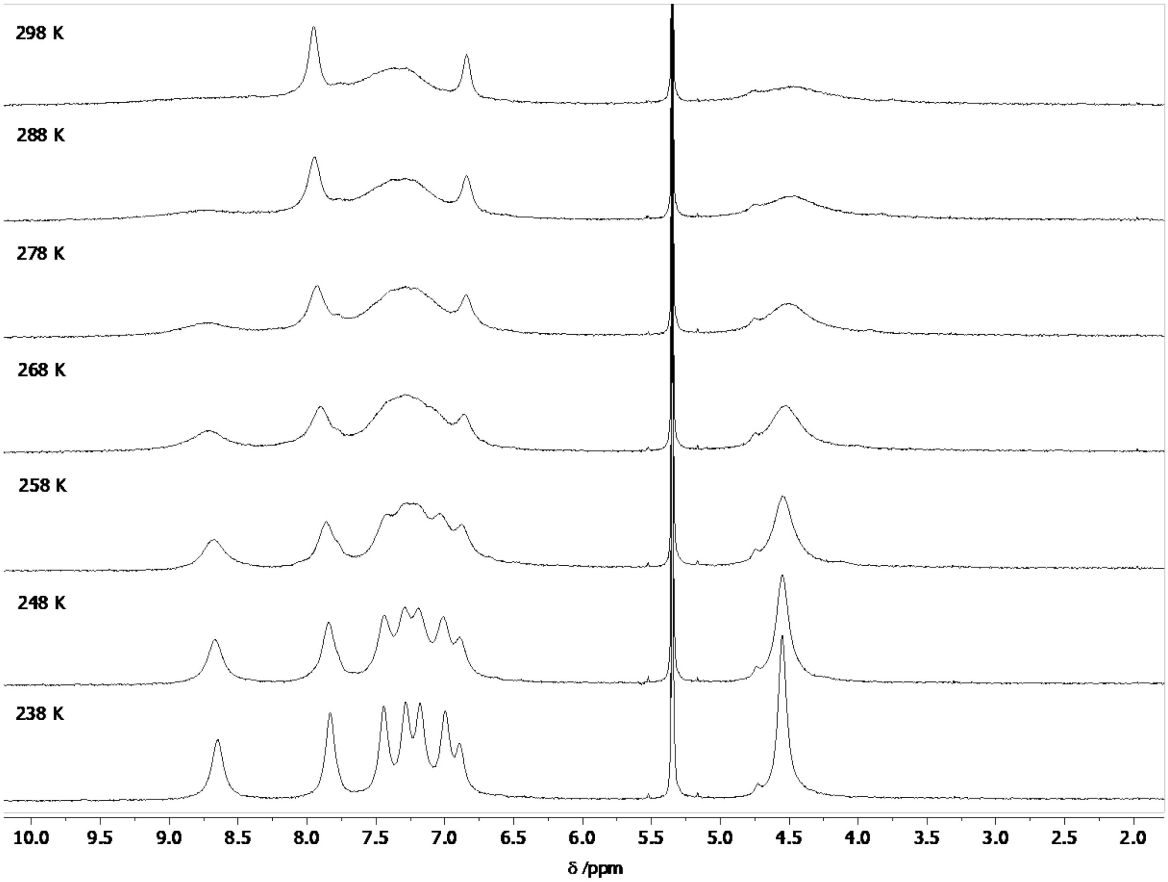

Figure S16. ^{1}H-NMR spectra (500 MHz) of CuCl(dpa^{H}) in d_2-DCM over the temperature range of 238–298 K.

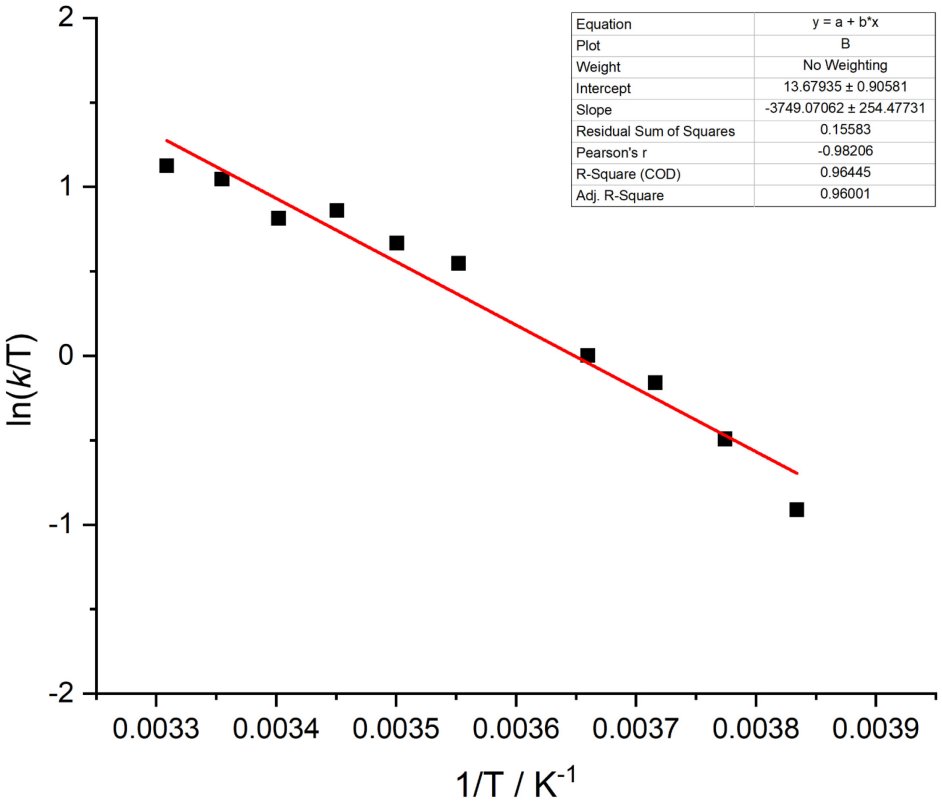

Figure S17. Plot of ln(k/T) versus 1/T (where k = rate constant and T = temperature in K) for the dynamic NMR process of CuCl(dpa^{H}) in d_2-DCM from 238–298 K. The shown linear fit was used to calculate the activation parameters listed in the main text via the Eyring equation (R^2 = 0.96445).

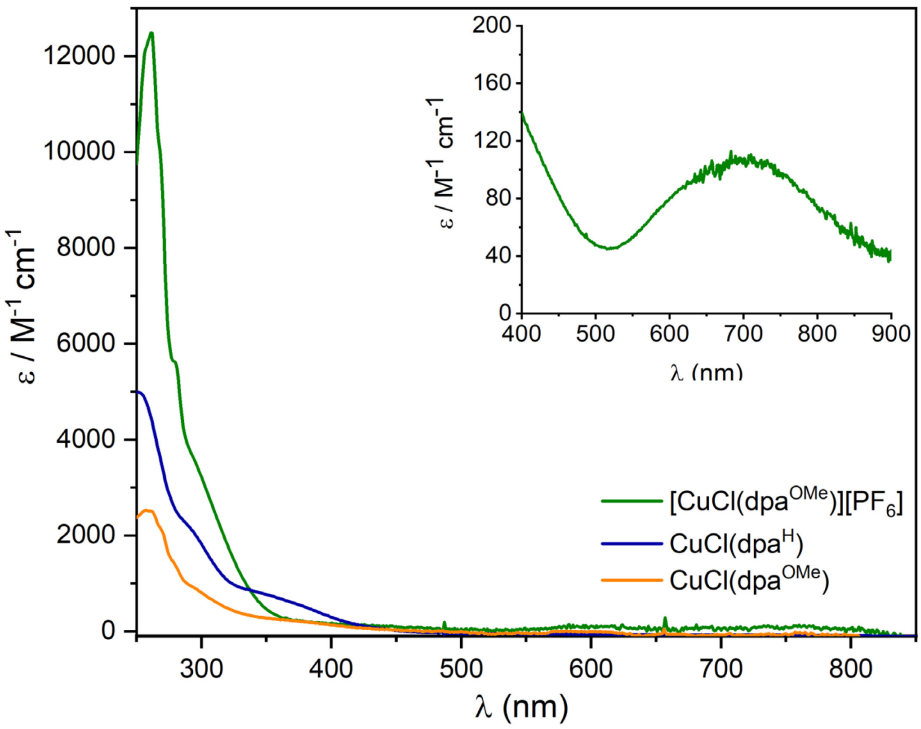

Figure S18. Extinction coefficient plots for [CuCl(dpa^{OMe})][PF_6] (green), CuCl(dpa^{H}) (blue) and CuCl(dpa^{OMe}) (orange) in DCM. Inset: Zoomed in region of [CuCl(dpa^{OMe})][PF_6] spectra from 400–900 nm.

References

1. J. Sandstrom, *Dynamic NMR Spectroscopy*, Academic Press, London, 1982.
2. M. Hasani, L. Nordstierna and A. Martinelli, *Phys. Chem. Chem. Phys.*, 2019, **21**, 22014–22021.
3. M. R. Willcott, *J. Am. Chem. Soc.*, 2009, **131**, 13180–13180.